REPORT DOCUMENTATION PAGE

Form Approved OMB NO. 0704-0188

1. REPORT DATE (DD-MM-YYYY)	2. REPORT TYPE	3. DATES COVERED (From - To)
30-12-2011	Final Report	25-Jun-2008 - 30-Sep-2011

4. TITLE AND SUBTITLE

Novel quantum states with exotic spin properties-
-Unconventional generalization of magnetism

5a. CONTRACT NUMBER
W911NF-08-1-0291

5b. GRANT NUMBER

5c. PROGRAM ELEMENT NUMBER
611102

6. AUTHORS

Yi Li, Hsiang-hsuan Hung, Zi Cai, Congjun Wu, Wei-Cheng Li, Dan Arovas

5d. PROJECT NUMBER

5e. TASK NUMBER

5f. WORK UNIT NUMBER

7. PERFORMING ORGANIZATION NAMES AND ADDRESSES

University of California - San Diego
Office of C & G Administration
The Regents of the Univ. of Calif., U.C. San Diego
La Jolla, CA 92093 -0934

8. PERFORMING ORGANIZATION REPORT NUMBER

9. SPONSORING/MONITORING AGENCY NAME(S) AND ADDRESS(ES)

U.S. Army Research Office
P.O. Box 12211
Research Triangle Park, NC 27709-2211

10. SPONSOR/MONITOR'S ACRONYM(S)
ARO

11. SPONSOR/MONITOR'S REPORT NUMBER(S)
54346-PH.17

12. DISTRIBUTION AVAILIBILITY STATEMENT

Approved for Public Release; Distribution Unlimited

13. SUPPLEMENTARY NOTES

The views, opinions and/or findings contained in this report are those of the author(s) and should not contrued as an official Department of the Army position, policy or decision, unless so designated by other documentation.

14. ABSTRACT

My group has investigated the unconventional meta-magnetic states in the Sr3Ru2O7 system, topological insulators, and superconductivity in iron-based superconductors. First, we constructed the microscopic mechanism of the nematic states in the Sr3Ru2O7 system based on its quasi-one-dimensional band structure. The calculated phase diagram agrees with the experimental observation. We performed the detailed theoretical analysis of the quasi-particle interference (QPI) spectroscopy of the STM measurement, which is in nice agreement with the

15. SUBJECT TERMS

unconventional metamagnetism, Sr3Ru2O7, topological insulators, iron based superconductors

16. SECURITY CLASSIFICATION OF:			17. LIMITATION OF ABSTRACT	15. NUMBER OF PAGES	19a. NAME OF RESPONSIBLE PERSON
a. REPORT	b. ABSTRACT	c. THIS PAGE			Congjun Wu
UU	UU	UU	UU		19b. TELEPHONE NUMBER 858-534-3325

Report Title

Novel quantum states with exotic spin properties-
-Unconventional generalization of magnetism

ABSTRACT

My group has investigated the unconventional meta-magnetic states in the Sr3Ru2O7 system, topological insulators, and superconductivity in iron-based superconductors. First, we constructed the microscopic mechanism of the nematic states in the Sr3Ru2O7 system based on its quasi-one-dimensional band structure. The calculated phase diagram agrees with the experimental observation. We performed the detailed theoretical analysis of the quasi-particle interference (QPI) spectroscopy of the STM measurement, which is in nice agreement with the experimental results. Second, we studied strong correlation effects in the 2D topological insulators by performing the sign-problem-free quantum Monte-Carlo simulations, and obtained the phase diagram. How the edge states are destabilized at an intermediate interaction strength is investigated. We have also constructed models of 3D topological insulators based on the generalization of Landau levels. The elegant analytical properties of Landau level provides a good starting point for the future study of fractional topological insulators in 3D. Third, we have investigated the unconventional superconductivity in iron-based superconductors. Time-reversal symmetry breaking states are proposed and the experimentally testable signatures are presented. We further provided a theory explanation of the anisotropic states observed in FeSe superconductors based on orbital ordering.

Enter List of papers submitted or published that acknowledge ARO support from the start of the project to the date of this printing. List the papers, including journal references, in the following categories:

(a) Papers published in peer-reviewed journals (N/A for none)

Received		Paper
2011/12/29 2:	15	Wei-Cheng Lee, D. P. Arovas, Congjun Wu. Quasiparticle interference in the unconventional metamagnetic compound Sr_{3}Ru_{2}O_{7}, Physical Review B, (05 2010): 0. doi: 10.1103/PhysRevB.81.184403
2011/12/29 1:	12	Wei-Cheng Lee, Shou-Cheng Zhang, Congjun Wu. Pairing State with a Time-Reversal Symmetry Breaking in FeAs-Based Superconductors, Physical Review Letters, (5 2009): 0. doi: 10.1103/PhysRevLett.102.217002
2011/12/29 1:	11	Joseph Maciejko, Chaoxing Liu, Yuval Oreg, Xiao-Liang Qi, Congjun Wu, Shou-Cheng Zhang. Kondo Effect in the Helical Edge Liquid of the Quantum Spin Hall State, Physical Review Letters, (06 2009): 0. doi: 10.1103/PhysRevLett.102.256803
2011/12/29 1:	10	. Theory of unconventional metamagnetic electron states in orbital band systems, Physical Review B, (09 2009): 0. doi:
2011/12/29 1:	9	Guang-Ming Zhang, Congjun Wu, Dong Zheng. Particle-hole symmetry and interaction effects in the Kane-Mele-Hubbard model, Physical Review B, (11 2011): 0. doi: 10.1103/PhysRevB.84.205121
2011/12/29 1:	8	Can-Li Song, , Yi-Lin Wang, , Peng Cheng, , Ye-Ping Jiang, , Wei Li, , Tong Zhang, , Zhi Li, , Ke He, , Lili Wang, , Jin-Feng Jia, , Hsiang-Hsuan Hung, , Congjun Wu, , Xucun Ma, , Xi Chen, , Qi-Kun Xue . Direct Observation of Nodes and Twofold Symmetry in FeSe Superconductor, Science, (06 2011): 0. doi:
2010/01/29 1:	7	W. Lee, C. Wu, D. Arovas, S. Zhang. Quasiparticle interference on the surface of the topological insulator Bi2Te3, Physical Review B, (12 2009): . doi:
2010/01/29 1:	6	W. Lee, C. Wu. Spectroscopic Imaging Scanning Tunneling Microscopy as a Probe of Orbital Structures and Ordering, Physical Review Letters, (10 2009): . doi:
2010/01/29 1:	5	W. Lee, C. Wu. Theory of unconventional metamagnetic electron states in orbital band systems, Physical Review, (09 2009): . doi:
2009/02/04 1:	2	Congjun Wu, . Orbital Analogue of the Quantum Anomalous Hall Effect in p-Band Systems, , ( ): . doi:

TOTAL: 10

Number of Papers published in peer-reviewed journals:

(b) Papers published in non-peer-reviewed journals (N/A for none)

Received	Paper

TOTAL:

Number of Papers published in non peer-reviewed journals:

(c) Presentations

1) Institute of Physics, Chinese Academy of Sciences, “Unconventional metamagnetic, transition and orbital ordering in transition metal oxides”, August 2011 (presented by C. Wu).

2) Topological insulator workshop at Kavli Institute of Theoretical Physics, University of California, Santa Barbara, "Isotropic Landau Levels of Relativistic and Non-Relativistic Fermions in 3D Flat Space", Sept 30, 2011 (presented by C. Wu)

3) Toplogical insulator workshop at Kavli Institute of Theoretical Physics, China, Isotropic Landau Levels of Relativistic and Non-Relativistic Fermions in 3D Flat Space", Aug 25, 2011 (presented by group member, Yi Li)

4)Department of Physics, University of California, Santa Crutz, condensed matter seminar, “Unconventional metamagnetic transition in the t2g orbital system of Sr3Ru2O7”, May 21, 2010. (Presented by C. Wu)

5) Quantum simulation workshop, University of Science and Technology of China, "“Unconventional metamagnetic transition in the t2g orbital system of Sr3Ru2O7”, July 30, 2010. (Presented by C. Wu)

6) Institute of Physics, Chinese Academy of Sciences, “Unconventional metamagnetic transition in the t2g orbital system of Sr3Ru2O7”, Aug. 17, 2010. (Presented by C. Wu)

7) Poster "Nematic Electron States and unconventional magnetism in Sr3Ru2O7 systems, International Conference on Strongly Correlated Electron Systems, Jun 27- July 2, Santa Fe. (Presented by C. Wu)

8) Contributed talk: "Unconventional meta-magnetism in transitional metal oxides", APS March meeting, Portland, March 2010. (Presented by by my group member W. C. Lee)

9)Time-Reversal Symmetry Breaking Pairing State in FeAs Based Superconductors, APS March Meeting in Pittsburgh, PA, Mar. 15-20, 2009. Presented by my group member Wei-Cheng Lee.

10) Poster (presented by Congjun Wu): Nematic Electron States and unconventional magnetism in Sr3Ru2O7 systems, New Directions in Low-Dimensional Electron Systems, KITP UCSB, Feb. 23-27, 2009.

11) Helical Luttinger liquid and the edge of quantum spin Hall systems, KITP mini-workshop of topological insulators, Dec 9, 2008, presented by Congjun Wu.

12) Contributed talk: Possible Time-Reversal Symmetry Breaking Pairing State in FeAs Based Superconductors, California Condensed Matter Meeting, UC-Riverside, Nov. 1-2, 2008. Presented by Wei-Cheng Lee.

Number of Presentations: 0.00

Non Peer-Reviewed Conference Proceeding publications (other than abstracts):

Received	Paper

TOTAL:

Number of Non Peer-Reviewed Conference Proceeding publications (other than abstracts):

Peer-Reviewed Conference Proceeding publications (other than abstracts):

Received	Paper

TOTAL:

Number of Peer-Reviewed Conference Proceeding publications (other than abstracts):

(d) Manuscripts

Received	Paper	
2011/12/29 14	14	Yi Li, Kenneth Intriligator, Yue Yu, Congjun Wu. Isotropic Landau levels of Dirac fermions in high dimensions, arXiv.org:1108.5650 (12 2011)
2011/12/29 14	13	Yi Li, Congjun Wu. Three Dimensional Topological Insulators with Landau Levels, arXiv.org1103.5422 (03 2011)
2009/02/10 14	4	Wei Cheng Lee, Congjun Wu. Nematic Electron States Enhanced by Orbital Band Hybridization, ( )
2009/02/04 13	3	Congjun Wu, Ian Mordragon Shem. Exciton Condensation with Spontaneous Time Reversal Symmetry Breaking, ( )
2009/02/04 13	1	Wei-Cheng Lee, Shou-Cheng Zhang, Congjun Wu. Time Reversal Symmetry Breaking Pairing State in FeAs Based Superconductors, ( )

TOTAL: 5

Number of Manuscripts:

Books

Received	Paper

TOTAL:

Patents Submitted

Patents Awarded

Awards

1. “Outstanding Young Researcher Award” of Overseas Chinese Physics Association, 2008.

2. Alfred P. Sloan Research Fellowship, 2008.

Graduate Students

NAME	PERCENT_SUPPORTED	Discipline
Hsiang-hsuan Hung	0.50	
Yi Li	0.00	
FTE Equivalent:	**0.50**	
Total Number:	**2**	

Names of Post Doctorates

NAME	PERCENT_SUPPORTED
Wei-Cheng Lee (21 months)	1.00
Zi Cai (9 months)	1.00
FTE Equivalent:	**2.00**
Total Number:	**2**

Names of Faculty Supported

NAME	PERCENT_SUPPORTED	National Academy Member
Congjun Wu (3 months/3 years)	1.00	
FTE Equivalent:	**1.00**	
Total Number:	**1**	

Names of Under Graduate students supported

NAME	PERCENT_SUPPORTED
FTE Equivalent:	
Total Number:	

Student Metrics

This section only applies to graduating undergraduates supported by this agreement in this reporting period

The number of undergraduates funded by this agreement who graduated during this period:	2.00
The number of undergraduates funded by this agreement who graduated during this period with a degree in science, mathematics, engineering, or technology fields:.....	1.00
The number of undergraduates funded by your agreement who graduated during this period and will continue to pursue a graduate or Ph.D. degree in science, mathematics, engineering, or technology fields:.....	0.00
Number of graduating undergraduates who achieved a 3.5 GPA to 4.0 (4.0 max scale):	0.00
Number of graduating undergraduates funded by a DoD funded Center of Excellence grant for Education, Research and Engineering:	0.00
The number of undergraduates funded by your agreement who graduated during this period and intend to work for the Department of Defense	0.00
The number of undergraduates funded by your agreement who graduated during this period and will receive scholarships or fellowships for further studies in science, mathematics, engineering or technology fields:	0.00

Names of Personnel receiving masters degrees

NAME
Total Number:

Names of personnel receiving PHDs

NAME
Hsiang-hsuan Hung
Total Number: 1

Names of other research staff

NAME	PERCENT_SUPPORTED
FTE Equivalent:	
Total Number:	

Sub Contractors (DD882)

Inventions (DD882)

Scientific Progress

Technology Transfer

Scientific progress and accomplishments

Congjun Wu, Department of Physics, University of California, San Diego

We present our research for the ARO award W911NF0810291 with the title "*Novel quantum states with exotic spin properties - Unconventional generalizations of magnetism*" in the entire supporting period (Jul. 2008- Sept. 2011). My group has made significant progress in several directions related to the proposed results. We present our research on the microscopic mechanism on the nematic states observed in $Sr_3Ru_2O_7$ in Sect. 1. The study of strong correlation effects in topological insulators is presented in Sect. 2. The study of a novel topological insulators based on high dimensional Landau levels is presented in Sect. 3. In Sect. 4, we present our study on the iron-based superconductivity. The summary of important results in given in Sect. 5.

Under the support by ARO, we have an excellent publication record in high profile research journals. We have published one article in Science, four articles in Physical Review Letters, four articles in Physical Review B, and three papers under review at Physical Review.

Below we will describe the progress in each direction.

1 Unconventional magnetism in $Sr_3Ru_2O_7$

We extended our idea of unconventional magnetism of the Fermi liquid theory [1, 2] to orbital band systems, and applied it for the nematic metamagnetic state observed in the strontium ruthenate material $Sr_3Ru_2O_7$ in A. Mackenzie's group. The microscopic theory for the nematic metamagnetic transition was constructed [3]. This state is essentially the unconventional magnetic states we proposed in the *d*-wave channel with a partial spin polarization [1, 2]. In the realistic orbital band systems of $Sr_3Ru_2O_7$, it also induces orbital ordering. Furthermore, we performed the calculation to explain the experimentally observed the quasi-particle interference pattern of the STM spectroscopy in $Sr_3Ru_2O_7$ measured by J. C. Davis's group [4, 5]. We also investigated the thermodynamic properties in the nematic regime [6], which was measured in A. Mackenzie's group [7, 8].

1.1 The key questions of the nematic states in $Sr_3Ru_2O_7$

In the past decade, the nematic metamagnetic states observed in the external magnetic field have aroused a great deal of research interest in the condensed matter community. When the *B*-field perpendicular is applied to the *ab*-plane between 7.8 and 8.1 Tesla, the transport properties exhibit a strong spontaneous in-plane anisotropy along the *a* and *b*-axis [9, 10, 11, 12, 13, 14, 15, 16].

This effect is of electronic origin because the lattice distortion observed is negligible. It has been interpreted as a nematic state with the anisotropic distortion of the Fermi surface of the majority spin polarized by the external magnetic field in Ref. [10]. Two key questions have still not been answered satisfyingly in previous theory work. First, $Sr_3Ru_2O_7$ is a t_{2g}-band (d_{xz}, d_{yz}, and d_{xy}) system with the active 4*d*-orbitals of Ru. The d_{xz} and d_{yz}-orbitals extend in the *xz* and *yz* plane, respectively, thus they behave quasi-one dimensional in the *ab*-plane. The d_{xy}-orbital lies inside the *ab*-plane, and its band structure is two-dimensional. Which bands are responsible for the nematic behavior? Second, the nematic metamagnetic states require strong exchange interactions in the *d*-wave channel, while the usual exchange interaction from Coulomb repulsion is dominate in the *s*-wave channel. How to reconcile this discrepancy?

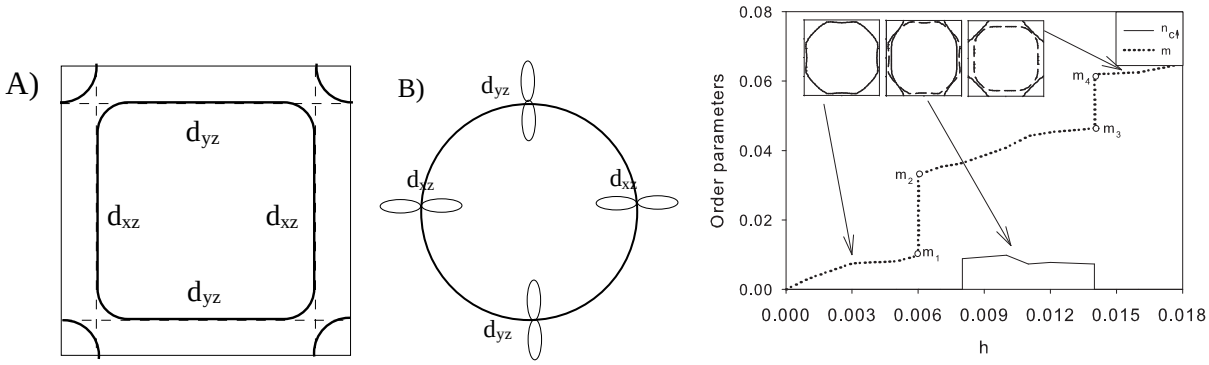

Figure 1: A) The hybridized quasi-1D bonding bands of d_{xz} and d_{yz}. As moving around the large Fermi surface, the orbital configuration exhibits a d-wave pattern, varying from $d_{xz} \to d_{yz} \to d_{xz} \to d_{yz}$. B) An idealized Fermi surface by rounding off the large Fermi surface in A). C) Self-consistent calculation results of the spin magnetization m (the dotted line) and the the nematic order parameter n (the solid line) *versus* the external magnetic field h. The nematic ordering develops between two consecutive metamagnetic transitions. The topologies of Fermi surface in each phases are sketched in the insects, where the solid and dashed lines represent the Fermi surface of the majority and the minority spin bands.

We have provided a natural answer by extending our previous theory of unconventional magnetism into multi-band systems in Ref. [3]. We point out that it is the hybridized *quasi-one-dimensional* d_{xz} and d_{yz} bands that are responsible for the nematic ordering based on the following reasoning. The nematic metamagnetic state is only observed in the bilayer compound $Sr_3Ru_2O_7$, but not in the monolayer compound Sr_2RuO_4, both of which are the t_{2g}-orbital systems. The key difference in electronic structures between them is the bilayer splitting, which is prominent for the quasi-one dimensional bands of d_{xz} and d_{yz} but small for the two-dimensional bands of d_{xy}. It is natural to expect that the spontaneous nematic behavior occurs in the bands of d_{xz} and d_{yz} and is accompanied by an orbital ordering. Furthermore, our mechanism based on the quasi-one dimensional band naturally generates the exchange interaction in the d-wave channel. The orbital band hybridization between d_{xz} and d_{yz} shifts a significant spectra weight of the exchange interaction into the d-wave channel, thus the nematic ordering can arise from the conventional multi-band Hubbard interactions.

1.2 Our mechanism – unconventional magnetism in the d_{xz} and d_{yz}-bands

We present below a heuristic picture to illustrate how orbital hybridization between the d_{xz} and d_{yz} band enhances the d-wave channel exchange interaction. We first review the exchange interaction in the usual single band system in the Landau Fermi liquid theory. At the Hartree-Fock level it is expressed as $f^a(\vec{p}_1, \vec{p}_2) = -\frac{1}{2}V(|\vec{p}_1 - \vec{p}_2|)$, where a represents the spin channel interaction, $V(\vec{p})$ is the Fourier transform of the two-body interaction $V(|\vec{r}_1 - \vec{r}_2|)$, say, the Coulomb interaction. The high partial wave channel components of $V(\vec{q})$ are usually weak, thus the condition for unconventional magnetism is more stringent than the usual the s-wave channel ferromagnetism.

This situation is significantly changed in the hybridized d_{xz} and d_{yz} quasi-one dimensional bands presented above. Without loss of generality, let us round off the large Fermi surface depicted in Fig. 2 A to a circle as in Fig. 2 B assuming that the single particle orbital configuration takes

the form of $|\psi_\sigma(\vec{p})\rangle = e^{i\vec{p}\cdot\vec{r}}u(\vec{p})\otimes\chi_\sigma$, where $u(\vec{p}) = (\cos\phi_p|d_{xz}\rangle + \sin\phi_p|d_{yz}\rangle)$ is the Bloch wave function with the internal orbital configurations; ϕ_p is the azimuthal angle of $\vec{p}$; $\chi_\sigma(\sigma = \uparrow,\downarrow)$ are the spin eigenstates. The exchange interaction between electrons with the same spin is $-V(\vec{p}_1 - \vec{p}_2)|\langle u(p_1)|u(p_2)\rangle|^2 = -V(\vec{p}_1 - \vec{p}_2)\cos^2(\phi_{p_1} - \phi_{p_2})$. Because of this factor of the inner product, the spin channel exchange interaction changes into

$$f^a(\vec{p}_1,\vec{p}_2) \quad = \quad -\frac{1}{4}[1+\cos 2(\phi_{p_1}-\phi_{p_2})]V(\vec{p}_1-\vec{p}_2). \tag{1}$$

Therefore even if the bare interaction $V(\vec{p}_1 - \vec{p}_2)$ is dominated by the *s*-wave channel, the extra *d*-wave factor arising from the orbital hybridization shifts a significant weight into the *d*-wave channel.

With the above non-trivial band structure, we achieve the experimentally observed nematic metamagnetic state with the multi-band Hubbard interactions. These interactions, including the intra-orbital and inter-orbital repulsions and Hunds rule couplings, are natural interactions widely used to describe transition metal oxides. Thus we do not need artificial interactions as in Ref. [17, 18, 19]. The Hubbard interactions by themselves do not result in the exotic nematic states because their contribution is concentrated in the isotropic *s*-wave channel if there were no band hybridization. However, when projected into the hybridized d_{xz} and d_{yz} bands, Hubbard interactions acquire the *d*-wave channel component with a significant weight which is responsible for the nematic states. The phase diagram from the self-consistent calculation is presented in Fig. 2 C.

1.3 Spectroscopic imaging scanning tunneling microscopy (STM) as a probe to the nematic metamagnetic state

Quasi-particle interference (QPI) of the spectroscopic imaging STM has become a powerful method to investigate electronic structure and competing orders in strongly correlated systems [20, 21, 22, 23]. It is amazing that the real space local probe of STM can give rise to the electronic information of momentum space. It has the advantages of a high energy resolution and the ability to access unoccupied states above the Fermi energy. The process of the QPI analysis is as follows. First, the real space distribution of the local density of states around a single impurity is measured by STM with a high precision. Then its Fourier transform is performed, which reveals the momentum change during electron scattering processes. Positions with high spectra weight correspond to scattering wavevectors connecting regimes with high density of states in the iso-energy line in momentum space.

In the presence of nematic ordering, the Fermi surface exhibits anisotropic distortion. The four-fold rotational symmetry of the Fermi surface is broken into two-fold. This symmetry breaking nicely exhibits in the QPI pattern in which the stripes only extend along one particular direction as expected for a nematic order. Thus QPI provides a sensitive probe to the nematic ordering. In fact, this pattern has actually been seen in QPI spectra of the iron-pnictide compound $CaFe_2As_2$ in the $\alpha_{1,2}$-Fermi surfaces around the Γ-point by the same group of J. C. Davis [24]. These Fermi surfaces are of the nature of d_{xz} and d_{yz}, thus our above analysis also applies.

Recently, this technique has been applied to $Sr_3Ru_2O_7$ with 1% Ru sites substituted by Ti in Davis' group [25]. The Ti sites behave as scattering centers. The most prominent feature in their results is the characteristic square-box-like pattern. In our theory, this pattern is the key feature of the scattering from the nearly nested quasi one-dimensional bands of d_{xz} and d_{yz} [4]. Our work

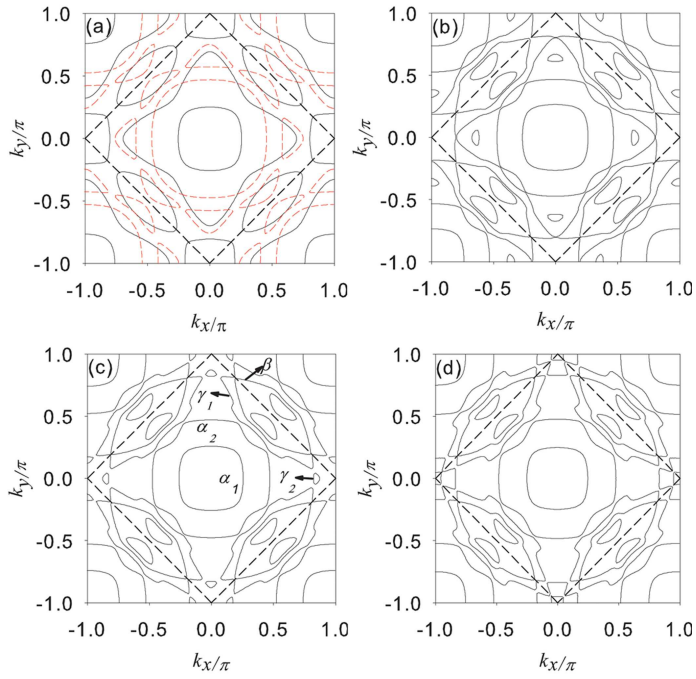

Figure 2: The Fermi surfaces of $Sr_3Ru_2O_7$ using the bilayer tight-binding model with different interlayer bias $V_{\rm bias}$ for (a) $V_{\rm bias}/t_0 = 0$, (b) $V_{\rm bias}/t_0 = 0.05$, (c) $V_{\rm bias}/t_0 = 0.1$, and (d) $V_{\rm bias}/t_0 = 0.15$. The thick dashed lines mark the boundary of half Brillouin zone due to the unit cell doubling induced by the rotation of octahedra oxygens. Fig. (a) represents the bulk Fermi surfaces without interlayer bias. The bonding ($k_z = 0$, black solid lines) and the anti-bonding bands ($k_z = \pi$, red dashed lines) could cross since k_z is a good quantum number. Fig. (c) fits the Fermi surfaces measured by ARPES best. Fermi surface sheets of α_1, α_2, γ_1, γ_2, and β are marked. From Ref. [27].

provides a theoretical support of a new detection method to the nematic metamagnetic state and orbital ordering.

The realistic band structure of $Sr_3Ru_2O_7$ We first constructed a tight-binding model to capture the complicated Fermi surface structures of the bilayer ruthenate compound of $Sr_3Ru_2O_7$, including its t_{2g}-orbital structure, the spin-orbit coupling, the bilayer splitting, and the staggered rotations of the RuO octahedra. The band parameters are chosen by fitting the calculated Fermi surfaces with those measured in the ARPES experiment performed by Shen's group [26]. We found that in order to explain the measured Fermi surface structures, an interlayer bias potential V_{bias} needs to be added between two RuO layers. This is because two top layers on the surface, which are sensitive to the ARPES measurement, are non-equivalent with different work functions. Such an effect is absent in the bulk due to the reflection symmetry between bilayers, which corresponds to $V_{bias} = 0$. The Fermi surface structures of $Sr_3Ru_2O_7$ with different values of the interlayer bias V_{bias} are presented in Fig. 2. As can be clearly seen, they are very complicated. Fig. 2 (c) is the best fit to the Fermi surfaces of the surface bilayer measured in ARPES. Fermi surface sheets marked with α_1, α_2, γ_1, γ_2, and β are observed in ARPES [26]. The γ_1 sheet has dominant 2-D d_{xy} orbital character; the small γ_2 sheets are hybridized between the d_{xy}-orbital and the quasi-1D $d_{xz,yz}$-orbital bands; the $\alpha_{1,2}$ sheets are mostly formed by quasi-1d $d_{yz,xz}$ orbitals.

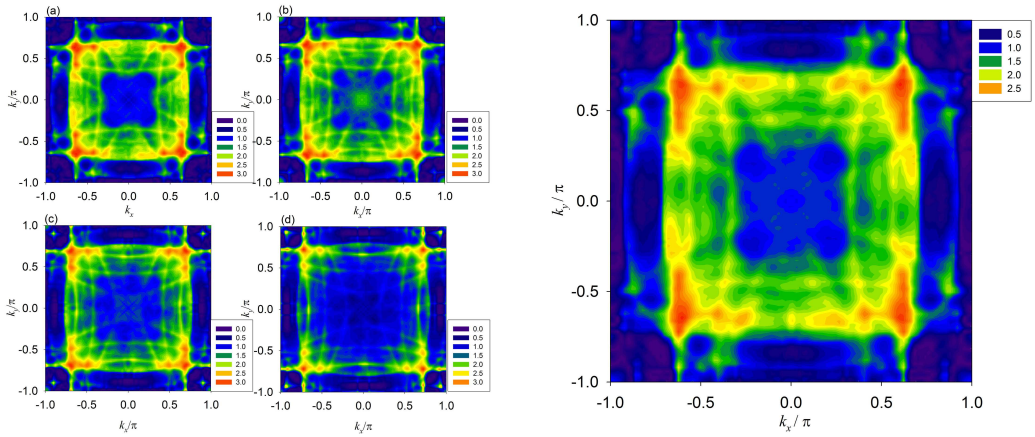

Figure 3: (LHS) QPI imagings at different values of bias (a) $E = 0$, (b) $E = -0.03$, (c) $E = -0.06$, and (d) $E = -0.1$. The main features are similar because the Fermi surfaces of $\alpha_{1,2}$ are relatively insensitive to E throughout this energy range. (RHS) The QPI imagings with the nematic order. The breaking of the four-fold symmetry to the two-fold symmetry is clearly seen. From Ref. [27].

The QPI spectra Based on the above band structure, we perform the T-matrix calculation for the QPI spectra with different values of the STM bias as presented in Fig. 3 (LHS). Our calculation exhibits the hollow square-box-like feature which agrees well with the experimental observation [25]. This dispersion of the QPI spectra with varying the STM bias is also qualitatively consistent with the experimental results. This square-box-like feature arises from the scattering from the nearly nested quasi-one-dimensional bands of the $\alpha_{1,2}$. The brightest spots at the corners come from the quasi-1D components of the small γ_2-bands. These bands are close to the van Hove singularity, and thus their scatterings are enhanced.

QPI as a probe to the nematic metamagnetic state The experiment performed by Davis' group on $Sr_3Ru_2O_7$ so far is in the zero magnetic field, which is out of the nematic phase, thus no 4-fold symmetry breaking effects were observed. In a previous paper [5], we have shown that the QPI is a sensitive method to detect the nematic ordering, which exhibits as the 4-fold symmetry breaking into the 2-fold symmetry. In fact, this pattern has actually been seen in the QPI spectra of the iron-pnictide compound $CaFe_2As_2$ in the $\alpha_{1,2}$-Fermi surfaces around the Γ-point in the same experiment group [28].

In our new paper [27], we calculated the QPI pattern in the nematic state in $Sr_3Ru_2O_7$ as depicted in Fig. 3 (RHS). In spite of the complicated band structures, the symmetry breaking pattern from the 4-fold to 2-fold is clearly seen. This feature can be tested in future experiments.

1.4 Thermodynamic properties of the unconventional metamagnetic states of $Sr_3Ru_2O_7$

Rost *et. al.*[7, 8] measured the entropy and specific heat near the metamagnetic transition and found divergences near as $C/T = A[(H - H_c)/H_c]^{-\alpha}$ with the exponent $\alpha = 1$. This feature has been interpreted as the signature of strong correlation physics of quantum criticality. Another puzzling is that the boundary of the nematic regime in the $T - H$ phase diagram has the "muffin" shape, i.e., increasing temperatures can drive the transition from the isotropic phase to the nematic phase. This means that the nematic phase has higher entropy than the isotropic phase at low temperatures.

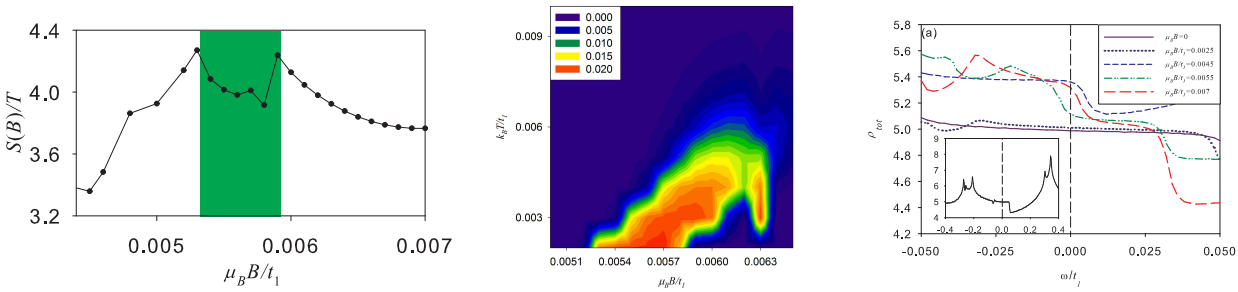

Figure 4: (LHS) The entropy landscape represented by the quantity $S(B)/T$ in unit of k_B^2/t_1 within the range of $0.0045 \leq \mu_B B/t_1 \leq 0.007$. A sudden increase near the nematic region (green area) is clearly seen. (Middle) Phase diagram at finite temperatures. Magnitudes of the nematic ordering are represented by the color scales. The re-entry of the nematic order at higher temperature is seen at fields between $0.0058 < \mu_B B/t_1 < 0.0063$. (RHS) The total DOS $\rho_{tot}(\omega)$ as a function of $\mu_B B$. $\rho_{tot}(\omega)$ does not follow the rigid band picture and $\rho_{tot}(\omega = 0)$ has a sudden increase near the nematic region. Inset: the total DOS at zero field for a wider range of $|\omega|/t_1 \leq 0.4$. The peaks corresponding to van Hove singularities are near $\omega/t_1 \approx -0.2$ and $\omega/t_1 \approx 0.35$.

Motivated by the observation that at low temperatures, both the nematic and isotropic phases are Fermi liquids from the resistivity-temperature measurements, we feel that the self-consistent mean-field theory (MFT) is sufficient to capture the essential physics. In our new paper [6], we performed the self-consistent MFT calculations for the thermodynamic quantities by taking into account the competition between ferromagnetic and nematic orderings, which qualitatively agree with the experimental results.

Entropy and DOS near the nematic region The entropy *v.s.* the Zeeman energy are plotted in Fig. 4 (LHS). The increase of the entropy towards the nematic regime and its non-monotonic behavior in the nematic regime are in agreement with experiments, which are combined effects of van Hove singularity of DOS and interaction. The calculated $H - T$ phase diagram is plotted in Fig. 4 (Middle), the shape of the phase boundary on the high-field side agrees with the experiment results, which means that increasing temperatures can drive the system into the nematic phase. This results are consistent with the entropy plotted in Fig. 4 (LHS), which shows that the entropy is larger in the nematic phase than the isotropy phase at the boundary of high field side. However, our calculation for the phase boundary of the low-field side does not agree with experiments.

Furthermore, we also calculated the density of states *v.s.* Zeeman energy, which shows that the increase of density of states when the field is in the nematic regime as presented in Fig. 4 (RHS). The density of states cannot be described as a rigid Zeeman shift in agreement with experiments. This is a result of spin-orbit coupling effect.

In-plane B field induced anisotropy Another puzzle remains to be explained is the correlation between transport anisotropy and the in-plane component of the B-field measured in experiments [11]. Suppose with an in-plane B-field along the x-axis, the resistivity measurements show that the easy axis is along the y-direction. As pointed out by Raghu *et al.* [29], an uniform nematic state actually does not exhibit much anisotropy in the charge transport. The point is that the nematic phase is mostly associated with the states near the van Hove singularity whose Fermi velocities are too small to have sizable contribution to the transport properties. Therefore the observed anisotropic resistivity is mostly likely due to the scatterings between nematic domains. However, it is still not

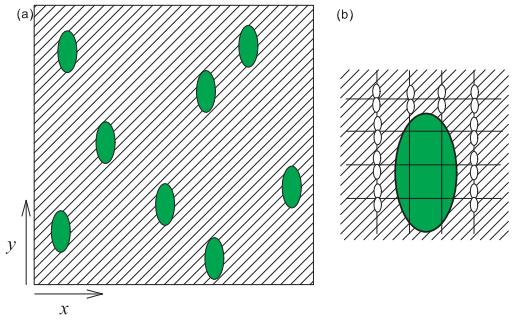

Figure 5: Illustration of the energetically-favored domain structures as the in-plane magnetic field is along $\hat{x}$ axis. When the in-plane magnetic field is weak, the phase with the preferred d_{yz}-orbital are dominant (shaded areas) and high-energy domains with the d_{xz}-orbital (green ovals) could exist. (b) The domain walls extend longer in $\hat{y}$ direction because it costs less energies if less $\hat{y}$- than $\hat{x}$- bonds are broken in the d_{yz}-orbital ordered background. The white oval represents the wave function of d_{yz} orbital on each site. The current flows much more easily along $\hat{y}$-axis than $\hat{x}$-axis since the electrons suffer less domain scatterings hopping along this direction. As the in-plane magnetic field is strong, these high-energy domains vanish, thus there is no longer an easy axis for the current flow.

clear why the easy axis of charge transport is perpendicular to the in-plane B-field.

We provide a natural explanation below based on the anisotropic spatial extension of the domain walls as explained below as depicted in Fig. 5. Assuming the B-field lying in the xz-plane, the in-plane (xy) orbital Zeeman energy reads $H_{in-plane} = -\mu_B B \sin\theta \sum_{i,a} L_{x,ia}$, which couples the d_{xy} and d_{xz}-orbitals and breaks the degeneracy between the d_{xz} and d_{yz}-orbitals. Since the d_{xy}-orbital has lower on-site energy due to the crystal field splitting than that of d_{xz}, the d_{xz}-orbital bands are pushed to higher energy than d_{yz}-orbital bands by this extra coupling. As a result, the nematic state with preferred d_{yz}-orbitals has lower energy in the homogeneous system. At small angles of θ, domains with preferred d_{xz}-orbitals could form as depicted in Fig. 5 (a) as meta-stable states, which occupy less volume than the majority domains. Let us consider the shape of the domain walls. Because of the quasi-1D features, the horizontal (vertical) domain wall breaks the bonds of the $d_{yz}(d_{xz})$-orbital as depicted in Fig. 5 (b), respectively. Since the d_{yz}-orbital is preferred by $H_{in-plane}$, the horizontal domain wall costs more energy. Consequently, the domain structure illustrated in Fig. 5 (a) with longer vertical walls than the horizontal walls is energetically favored, and causes the easy axis of y for the current flow.

2 Strong interaction effects in the Kane-Mele model of topological insulators

The study of topological insulators (TI) in both two dimensions (2D) and three dimensions (3D) has become a major focus of condensed matter physics [30, 31, 32, 33, 34, 35, 36, 37, 38, 39, 40, 41, 42]. The quantum Hall systems are the prototype of topological insulators, which breaks time-reversal (TR) symmetry and whose magnetic band structure is characterized by the integer Chern number. In contrast, these new TIs maintain TR symmetry, and their band structures are characterized by the nontrivial Z_2-index for both 2D and 3D systems. On the edge of the 2D topological insulators, odd number channels of helical edge modes appear. On the surface of the 3D

topological insulators, odd number of surface Dirac cones appear. Both of them are stable against disorder scatterings. However, interaction effects in topological insulators have not been paid much attention yet. Although we expect that topological insulators remain stable at weak interactions, their stability under intermediate and strong interactions is an important open question.

Our previous work of Ref. [43] is one of the first two papers explicitly addressing this question (the other one is by J. Moore *et al.* posted at the same time [44]). The main result is that the Z_2 argument provided by Kane and Mele [33] needs reconsideration in the presence of interactions. Let us consider the 1D helical edge modes of the 2D TIs, although the single particle backscattering is forbidden by TR symmetry, the two-particle correlated backscattering are allowed by TR symmetry. The two-particle backscattering is an interaction effect. Under strong repulsive interactions, its effects are non-perturbative and can gap out the edge modes by spontaneously breaking TR symmetry. In other words, the helical edge modes become unstable. Concrete criteria for the stability of the helical edge modes were given in terms of the phenomenological Luttinger parameters based on the field theoretical analysis of bosonization.

2.1 Sign problem free QMC simulation to the Kane-Mele-Hubbard model

Based on our past analytical work, we further performed the numerical simulations of quantum Monte Carlo (QMC) for the quantitative results of strong interaction effects in topological insulators [45]. Our work is one of the first two papers using QMC to study the interaction effects in topological insulators (The other one is by Assaad's group [46]. These two works are independent from each other).

QMC plays an important role in the study of strong correlation effects of fermions, and is currently the only scalable numerical method generating exact results in 2D under suitable conditions. However, QMC suffers from the notorious "*sign problem*" for most fermion systems. This problem is the major obstacle for QMC to apply in strongly correlated systems. It refers to the fact that the amplitudes of a quantum process of fermions are usually not positive-definite, thus cannot be directly interpreted as classic probability. If the "sign problem" appears, numerical errors grow exponentially as increasing sample size and decreasing temperature and QMC fails. Under certain situations, for example, the Hubbard model in the bipartite lattice at half-filling, the sign problem disappears due to the particle-hole symmetry. In this case, conclusive results can be drawn from the high precession simulations. A celebrated result is the existence of the antiferromagnetic (AFM) long-range-order at zero temperature in the 2D square lattice [47].

Fortunately, we have proved that for the prototype model for the 2D TIs, the Kane-Mele model [33] with the augmentation of the Hubbard interaction, the sign problem is absent. This is counter-intuitive: the free part of the Kane-Mele-Hubbard model involves the next-nearest-neighbor (NNN) hopping in the honeycomb lattice. Usually, the NNN hopping breaks the particle-hole symmetry of the Hubbard model and leads to the sign problem and the failure of QMC. Nevertheless, in the case that the NNN hopping is purely imaginary, the Kane-Mele-Hubbard model is in fact particle-hole symmetry at half-filling.

Phase diagram of the Kane-Mele-Hubbard model using QMC Our results from QMC simulations are depicted in Fig. 6 LHS. U is the Hubbard interaction; λ is the spin-orbit coupling strength; t is the hopping amplitude. Clearly as U/t goes large, the system finally goes into long-range-ordered antiferromagnetic (AFM) phase whose boundary is marked. The AFM phase is a topologically trivial phase whose bulk state breaks TR symmetry. There are no non-trivial gapless

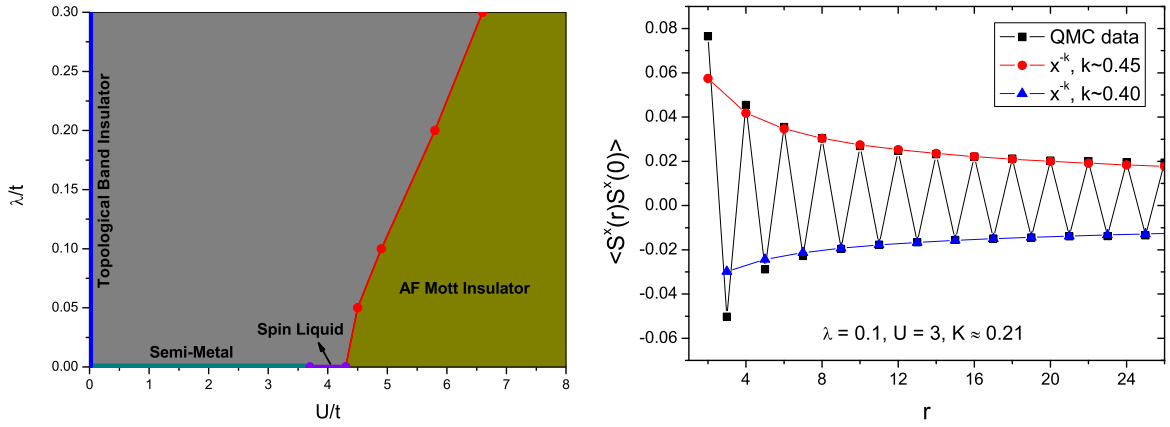

Figure 6: Left hand side (LHS): A plot of the phase diagram of the Kane-Mele-Hubbard model from our QMC simulations. The magnetic phase boundary is marked. The line of $\lambda = 0$ corresponds to the case of pure Hubbard model in the honeycomb lattice that was simulated in Ref. [48] by Meng *et al.*. Right hand side (RHS): The two-point equal-time spin correlation function $\langle G|S_x(\vec{r})S_x(\vec{r}')|G\rangle$ along the zig-zag edge with $\lambda = 0.1$ and $U = 3$. The length of the zig-zag edge is 2×34 and the width of the ribbon is 4. Because the zig-zag edge contains the sites of both A and B sub-lattices, the fitted decay powers are slightly different. We use their average value to obtain the Luttinger parameter $K \approx 0.21$.

edge modes in the AFM phase. Due to spin-orbit coupling, the spin $SU(2)$ symmetry is explicitly broken. The AFM moments favor lying in the xy-plane, thus it is in the XY-class.

There is a large portion in the phase diagram at small and intermediate values of U/t in which the system remains paramagnetic. Apparently, TR symmetry is maintained in the paramagnetic states. At $U/t = 0$, the system is non-trivial as the topological band insulator. But the question is that whether all the regime of the paramagnetic state is topologically non-trivial. Naively, one would expect that the system remains non-trivial with gapless edge modes until the bulk becomes AFM long-range-ordered. Here we will show that this picture is incorrect.

Destabilization of the helical edge modes A major result of our QMC simulations is that the edges of the Kane-Mele-Hubbard systems can be nearly AFM long-range-ordered while the bulk remains paramagnetic. Because of the band gap inside the bulk, the interaction needs to be stronger than the bulk band gap to drive AFM. Nevertheless, edges are gapless at weak interactions due to the non-trivial band topology. Interaction effects are prominent in gapless systems, thus the AFM correlations are stronger along edges than in the bulk. It is reasonable to expect that edges develop AFM earlier while the bulk remains TR invariant and paramagnetic.

In Fig. 6 RHS, we calculate the spin-spin correlation functions along the edge, which shows the power-law correlations. This means the developing of the quasi-long-range order. The only reason that prevents the developing of true long-rang order is the conservation of S_z for the purpose to remove the sign problem. However, this feature is not required for the most general models of topological insulators. This extra $U(1)$ symmetry cannot be spontaneously broken in 1D edge systems due to a rigorous result of Winger-Mermin-Coleman theorem. Nevertheless, in the Fig. 6 RHS with an intermediate value of $U/t = 3$, the average decay power of the AFM two-point function is very small. Actually, from our previous analytical results, as long as the condition of S_z-conservation is released, the edge will be AFM long-range-ordered and gapped.

In our previous bosonization analysis, the decay power of the edge spin correlation function

is $2K$, where K is the phenomenological Luttinger parameter to describe the helical edge modes. At $K < \frac{1}{2}$, the two-particle backscattering term mentioned before becomes non-perturbative, and destabilizes the helical edge modes by developing the true long-range ordered AFM. Such a term in principle is allowed to exist because it maintains TR symmetry. Thus we can divide the above paramagnetic regime in Fig. 6 LHS into two parts according $K < \frac{1}{2}$ and $K > \frac{1}{2}$, respectively. The regime of $K > \frac{1}{2}$ corresponds to weak interactions in which the edge remains stable against the two-particle backscattering; while the regime of $K < \frac{1}{2}$ corresponds to intermediate interactions, in which the bulk remains paramagnetic and the edge is unstable under the two-particle backscatterings. A precise phase boundary between them requires more detailed numerical work. Nevertheless, we have shown that the case depicted in Fig. 6 already belongs to the intermediate interaction regime and the helical edge modes are unstable.

2.2 Kondo problem in the helical edge modes

Magnetic impurities have dramatic effects in transport properties known as Kondo effect [49, 50, 51, 52, 53, 54, 55]. The Kondo effect in the helical edge states of the 2D topological insulators is an important question both theoretical and experimental.

Initialed in a previous work [56] and continued in a recent paper [57] in collaboration with S. C. Zhang's group, we have performed a thorough study of the Kondo effect in the helical edges of topological insulators. We have performed a renormalization group analysis with new features brought by interactions. It is remarkable that the repulsive interactions shift the critical Kondo coupling constant to the ferromagnetic side, which means that Kondo singlet can be formed with both the antiferromagnetic and weak ferromagnetic couplings. After the formation of the Kondo singlet, it behaves like a spinless impurity, which can only cause phase shift to the edge electrons. We further calculated the edge conductance of the 2D topological insulator as a function of temperature in the presence of a magnetic impurity. At high temperatures, Kondo and/or two-particle scattering give rise to a logarithmic temperature dependence. At low temperatures, for weak Coulomb interactions in the edge liquid the conductance is restored to unitarity with unusual power-laws characteristic of a 'local helical liquid', while for strong interactions transport proceeds by weak tunneling through the impurity where only half an electron charge is transferred in each tunneling event.

3 Topological insulators from 3D isotropic Landau levels

Introduction If we recall the study of topological states in condensed matter physics, it starts from the 2D QHE systems with Landau levels (LL). Later on, topological states were generalized to systems with Bloch-wave band structures but not LLs [58], which were known as quantum anomalous Hall insulators. The research of the TR invariant topological insulators in 2D and 3D mainly focuses on Bloch-wave band structures with the non-trivial topological Z_2-index. However, the 3D TR invariant topological insulators based on LLs have not been studied before. Usually, LLs are based on the planar structure subjected to the external magnetic field, thus it is not easy to generalize to 3D. Nevertheless, we have made a breakthrough successfully generating LLs to 3D with the full rotational symmetry [59, 60].

Compared to the usual topological insulators with Bloch-wave band structures, LLs have apparent advantages. LLs are flat without dispersions, thus interaction effects are non-perturbative.

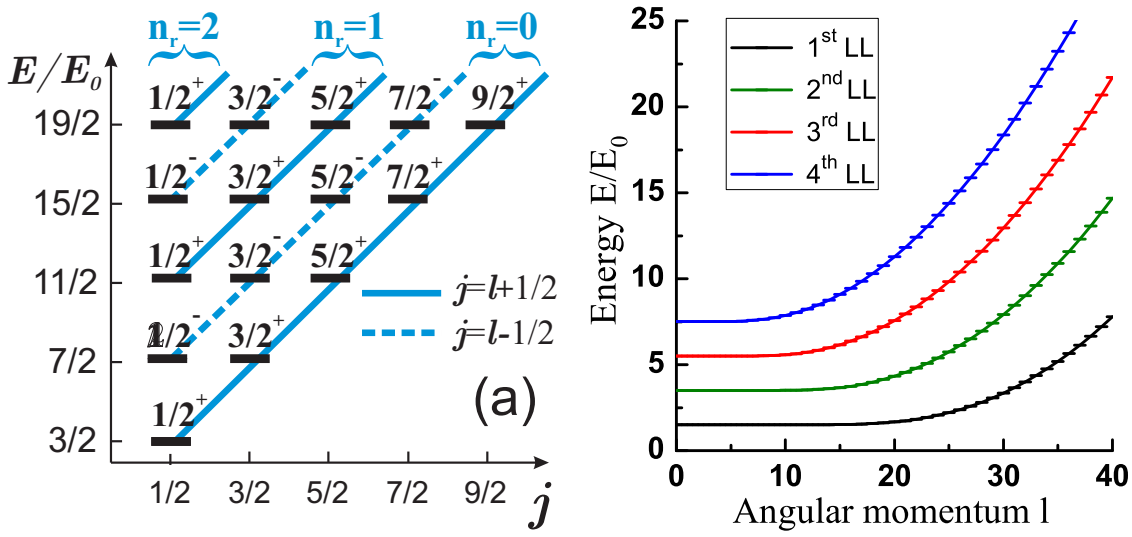

Figure 7: LHS) The eigenstates of the 3D harmonic oscillator labeled by total angular momentum $j_\pm = l \pm \frac{1}{2}$. Following the solid diagonal (dashed) lines, these states are reorganized into the fully rotational symmetric 3D Landau level sates with the positive (negative) helicity. RHS) Each LL contributes one branch of helical surface mode. The energy dispersion of the first four Landau levels *v.s.* $j_+ = l + \frac{1}{2}$. Open boundary condition is used for a ball with the radius $R_0/l_g = 8$.

Furthermore LLs possess beautiful analytical properties which do not exhibit in other band structure topological insulators. In fact, the study of the 2D fractional QHE effects is greatly benefited from the analytical properties of 2D LL. It is reasonable to expect fractional topological states in 3D with LLs, which will be our next research focus.

3D LLs from Aharanov-Casher coupling Our mechanism is actually very simple. Let us start from the 2D LL problem to gain some intuition, in which the $U(1)$ magnetic vector potential $\vec{A}$ minimally couples to the canonical momentum. In the symmetric gauge, $\vec{A} = \frac{1}{2}\vec{B} \times \vec{r}$. A nice observation is that the 2D LL Hamiltonian is just 2D harmonic potential plus the orbital Zeeman coupling. The 2D LL wavefunctions are just those of the 2D harmonic oscillator. The harmonic oscillator spectra exhibit the dispersion with respect to the orbital angular momentum m which is exactly canceled by the opposite dispersion of m from the orbital Zeeman coupling. As a result, each LL becomes dispersionless with respect to m. In other words, a different organization of the same set of harmonic oscillator wavefunctions, which are originally topologically trivial, gives rise to the topologically non-trivial LLs. However, the external magnetic field specifies a unique direction, thus it is not easy to generalize to 3D.

Instead, for the 3D case, we employ an Aharanov-Casher potential with the replacement of $\vec{B}$ by the three Pauli matrices $\vec{\sigma}$ as $\vec{A}_{\alpha\beta} = \frac{1}{2}\vec{\sigma}_{\alpha\beta} \times \vec{r}$, which is essentially an $SU(2)$ gauge potential. This Hamiltonian is actually the 3D harmonic oscillator plus spin-orbit coupling. The spectra of the 3D harmonic oscillators is depicted in Fig. 7 LHS as organized in the total angular momentum eigen-basis of $\vec{J} = \vec{L} + \vec{S}$. For each orbital angular momentum l, there are two different states with opposite helicities $j_\pm = l \pm \frac{1}{2}$. Depending on the sign of the spin-orbit coupling term, this term turns the eigenstates of the positive or negative helicity into 3D flat LLs. In particular, the 3D LLs also have a nice analytic structure: the spin-orbit coupled spheric harmonics replaces the role of azimuthal angular form factor $e^{im\phi}$ for the 2D LLs.

Helical surface modes – 3D strong topological insulators With the spherical open boundary condition, we find that each LL contributes a branch of helical surface mode. The calculated surface spectra are depicted in RHS of Fig. 7. At small values of l, the spectra remain flat because their wavefunctions are inside the bulk and thus are not sensitive to the boundary. As l increases, their wavefunctions begin to touch the open boundary, and thus their energy is pushed upward. Further analysis shows that the effective edge Hamiltonian for each LL is actually a Dirac Hamiltonian. Each filled LLs contribute one branch of helical Fermi surface. Thus if odd number of LLs are filled, the system is a 3D strong topological insulator.

Further developments We have further generalized the above 3D LLs for non-relativistic fermions to Dirac fermions, which can be considered as the generalization of the LLs of 2D graphene systems to the 3D systems with the full rotational symmetry. In fact, we have also generalized both of the 3D non-relativistic and relativistic LLs into arbitrary dimensions. Our next step of research will focus on interaction effects. Our dream is to find the 3D fractional topological insulator wavefunctions, i.e., the analogy of the Laughlin wavefunction in 3D, and the associated exotic many-body properties.

4 Superconductivity in iron-based superconductors

4.1 Time reversal (TR) symmetry breaking pairing states in iron-pnictide superconductors

The discovery of the iron-pnictide superconductors has attracted a great deal of attention [61, 62, 63, 64, 65, 66, 67]. They are novel systems with unconventional Cooper pairing, whose pairing symmetry remains highly debating. This problem is complicated by the structure of their multiple Fermi surfaces, which include the hole Fermi surfaces $\alpha_{1,2}$ around the Γ-point at $(k_x, k_y) = (0,0)$, and the electron Fermi surfaces $\beta_{1,2}$ around the $M_{1,2}$ points at $(\pi, 0)$ and $(0, \pi)$, respectively. Many theoretical proposals have suggested the fully-gapped $s_{\pm}$-wave state which preserves the 4-fold rotational symmetry [68, 69, 70, 71, 72]. Experimentally, the superfluid density obtained from the penetration depth measurements is insensitive to temperature, consistent with this picture [73, 74, 75]. Another competing pairing structure is $d_{x^2-y^2}$ as proposed by several groups [69, 76, 40]. In particular, it has been found that the $s_{\pm}$ and $d_{x^2-y^2}$ pairings are nearly degenerate in LaOFeP compounds [77].

Our proposal – time reversal symmetry breaking pairing Considering the competing nature between $s_{\pm}$ and $d_{x^2-y^2}$ pairings in iron-pnictide superconductors, we propose in Ref. [78] that their complex mixture $s_{\pm} + id_{x^2-y^2}$ with time reversal symmetry breaking can appear at low temperatures. As lowering the temperature, two consecutive superconducting transitions occur. The system first undergoes the transition to the time reversal invariant $s_{\pm}$-wave state, and then into the $s_{\pm} + id_{x^2-y^2}$ state by breaking time reversal symmetry. We also predicted various experimentally testable signatures, including spatial inhomogeneity induced supercurrents, and a novel collective mode. To our knowledge, our paper is the first one to study time reversal symmetry breaking Cooper pairing in iron-pnictide superconductors.

Unconventional superconductivity with time reversal symmetry breaking have been actively investigated in recent years. Previous examples include the Kerr rotation experiment of Sr_2RuO_4 consistent with the $p+ip$ pairing symmetry [79], and the neutron scattering experiments of $YBa_2Cu_3O_{6+x}$

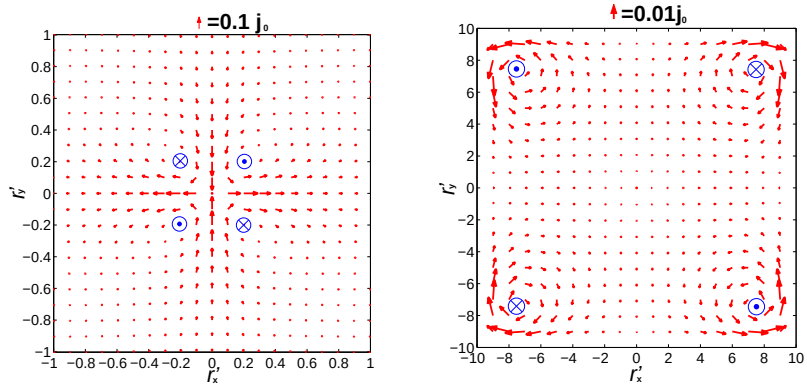

Figure 8: Spatial distributions of supercurrent induced by spatial inhomogeneity in the $s_{\pm}+id_{x^2-y^2}$ pairing state of iron-pnictide superconductors. LHS) The supercurrent pattern induced by a single impurity located at the center. RHS) The supercurrent pattern around in a square sample with open boundaries. The length of each arrow is proportional to the magnitude of the supercurrent. $\odot$ and $\otimes$ indicate the vorticities of the loop currents.

indicating the existence of the loop current ordering [80, 81, 82]. The possible time reversal symmetry breaking pairing state in iron-pnictide systems will add a new member to this exotic family if it is testified by experiments.

Spatial inhomogeneity induced supercurrent A novel experimentally testable consequence of the $s_{\pm}+id_{x^2-y^2}$ pairing is that spatial inhomogeneity induces supercurrent. In contrast, in the superconductor with either s-wave or d-wave pairing which preserves time reversal symmetry, spatial inhomogeneity only induces the variation of the pairing amplitude without affecting the pairing phase. Thus spatial inhomogeneity does not induce supercurrent simply because it does not breaks time reversal symmetry.

In the $s_{\pm}+id_{x^2-y^2}$ pairing state, time reversal symmetry is already broken. In the homogeneous systems, the relative phase between $s_{\pm}$ and $d_{x^2-y^2}$ components is fixed at $\pm\frac{\pi}{2}$, thus still no supercurrent exits. The $s_{\pm}$ and $d_{x^2-y^2}$ components can be coupled by the following gradient term in the Ginzburg-Landau free energy as

$$\gamma_{sd}\left\{\Delta_s^*(\partial_x^2-\partial_y^2)\Delta_d+c.c.\right\}, \tag{2}$$

which is allowed by all the symmetry requirement. In spatially inhomogeneous systems, the variation of the order parameters cause the inhomogeneity of the relative phase θ_{sd} due to the γ_{sd} term, which induces supercurrent even in the *absence* of external magnetic field.

We numerically solved the supercurrent patterns for both cases of a single impurity and a square sample with open boundaries. The results are depicted in Fig. 8 A and B, respectively. For the single impurity case, the magnitude of the supercurrent rapidly decays beyond the order of the healing length. The suppercurrent pattern is symmetric under a combined operation of time reversal and the rotation of $\pm 90^{\circ}$. Along the x and y-axis passing the impurity, the supercurrents flow along these axis and exhibit the pattern of "two in" and "two out", which is consistent with the reflection symmetry respect to the x and y-axis and the continuity condition. For the square sample, the continuity condition suppresses the supercurrent except at the four corners as depicted in Fig. 8 B. Each of four corners develop a circulating supercurrent loop whose chirality are staggered as

we move around the edges. This is also consistent with the combined symmetry operation of time reversal and the rotation of 90°. This circulating supercurrent can be detected by using the scanning SQUID.

Prediction of a novel collective resonance mode In the case that the $s_\pm$-pairing state wins over $d_{x^2-y^2}$ which occurs in many compounds in the iron-pnictide family, we predict a novel collective resonance mode. This mode excites the $d_{x^2-y^2}$ pairing in the background of $s_\pm$ and is described by the nematic operator $\hat{N}_d = 1/V\sum_k(\cos k_x - \cos k_y)c^\dagger_{\vec{k}\sigma}c_{\vec{k}\sigma}$. It lies in the particle-hole channel with the $d_{x^2-y^2}$ symmetry, which is precisely the electron excitations measured in the B_{1g} Raman mode. Because of the competing nature of the $s_\pm$ and $d_{x^2-y^2}$ pairings, this mode is a sharp low energy excitation below the superconducting gap. It is not damped by the quasiparticle excitations. A successful observation of such mode will be a demonstration of the completion between $s_\pm$ and $d_{x^2-y^2}$ pairings.

4.2 Orbital ordering the two-fold pairing symmetry in FeSe

One of the most important problem in the iron-based superconductors is the nature of the pairing symmetry. For most materials in the 1111-family, various experimental results agree with the nodeless extended $s_\pm$-wave pairing. However, in other families of 111 and 11, whether the pairing gap is nodal or nodeless is still controversial. On the other hand, many iron-based superconductors exhibit spontaneous nematic ordering which reduces the symmetry from the 4-fold rotational symmetry to 2-fold. A common reason is the developing of stripe-like antiferromagnetism whose wavevector is $(\pi,0)$ or $(0,\pi)$.

In collaboration with Q. K. Xue's experimental group at Tsinghua University in Beijing, my group helped them analyze the data, which yields important information on the pairing symmetry in the one of the simplest iron-based superconductors FeSe [83]. Using the methods of scanning tunneling microscopy and spectroscopy, their data reveal clear evidence for a gap function with nodal points. Furthermore, they also measured the vortex core tunneling spectra under external magnetic fields. Amazingly the vortex core are highly anisotropic breaking the 4-fold rotational symmetry. This anisotropy also exhibits in the real space imaging of the resonance scattering spectra around impurity sites, and in the quasi-particle interference pattern. Their paper is recently published in Science.

Different from previous iron-based materials in which the breaking of the 4-fold rotational symmetry to 2-fold is due to the striped antiferromagnetism. It is known that at ambient pressure, there is no antiferromagnetic instability in FeSe. In considering this fact, my group proposed that the anisotropy is due to orbital ordering – orbital-dependent reconstruction of electronic structure in FeSe. The apparent nodal structure in the gap function can be understood as the mixture between two different types of extended *s*-wave pairings including the nearest neighbor and the next-nearest neighbor pairings. If the nearest neighbor pairing dominates, the gap function is nodal. In FeSe, the orbital ordering also brings anisotropy to the gap functions. My group has also performed the theory calculation, which is in nice agreement with Prof. Xue's experimental data [84].

5 Summary of the most important results

We summarize the most significant results under the support of ARO as follows.

1. We constructed the microscopic theory for the unconventional meta-magnetic states observed in $Sr_3Ru_2O_7$ systems based on the quasi-1D band structures of d_{xz} and d_{yz} [3], calculated the quasi-particle interference pattern measured by J. C. Davis' group [5, 27], and investigated the thermodyanica quantities in such a system [6]. These results are published in Ref. [3, 5, 6, 27].

2. We studied interaction effects in topological insulators, including the quantum Monte Carlo (QMC) simulation of the phase diagram of the Kane-Mele-Hubbard model [45], and the Kondo effect in the helical edge states of the topological insulators [57]. We are one of the first two groups to performing the QMC calculation to the interacting topological insulators. The STM spectra in the helical surface states of Bi_2Te_3 are calculated in a good agreement with experiments [85]. We also generalize the usual Landau level to three dimensions, which is a 3D topological insulators with flat bands [59, 60]. These results are published in Ref. [57, 45, 59, 60].

3. We have also investigated the unconventional supercondutivity in iron-based superconductors. We are the first group to propose the time-reversal symmetry breaking pairing states in such a systems [78]. We also help the experimentalist to analyze their STM data in FeSe superconductor and find the evidence of orbital ordering [83]. A theory paper is also written to give a detailed explanation of the experiment [84].

References Cited

[1] C. Wu and S. C. Zhang. Dynamic generation of spin orbit coupling. *Physical Review Letters*, 93:36403, 2004.

[2] C. Wu, K. Sun, E. Fradkin, and S. C. Zhang. Fermi liquid instabilities in the spin channel. *Physical Review B*, 75:115103, 2007.

[3] Wei-Cheng Lee and Congjun Wu. Theory of unconventional metamagnetic electron states in orbital band systems. *Phys. Rev. B*, 80(10):104438, Sep 2009.

[4] Wei-Cheng Lee and Congjun Wu. Spectroscopic imaging scanning tunneling microscopy as a probe of orbital structures and ordering. arXiv.org:0906.1973, 2009.

[5] Wei-Cheng Lee and Congjun Wu. Spectroscopic imaging scanning tunneling microscopy as a probe of orbital structures and ordering. *Phys. Rev. Lett.*, 103(17):176101, Oct 2009.

[6] W. C. Lee and C. Wu. Microscopic theory of the thermodynamic properties of $sr_3ru_2o_7$. arXiv.org:1008.2468, 2010.

[7] A. W. Rost, R. S. Perry, J.-F. Mercure, A. P. Mackenzie, and S. A. Grigera. Entropy landscape of phase formation associated with quantum criticality in $sr_3ru_2o_7$. *Science*, 325:1360, 2009.

[8] A. W. Rost, A. M. Berridge, R. S. Perry, J.-F. Mercure, S. A. Grigera, and A. P. Mackenzie. Power law specific heat divergence in $sr_3ru_2o_7$. *Phys. Status Solidi B*, 247:513, 2010.

[9] S. A. Grigera, R. S. Perry, A. J. Schofield, M. Chiao, S. R. Julian, G. G. Lonzarich, S. I. Ikeda, Y. Maeno, A. J. Millis, and A. P. Mackenzie. Magnetic field-tuned quantum criticality in the metallic ruthenate sr3ru2o7. *Science*, 294:329, 2001.

[10] S. A. Grigera, P. Gegenwart, R. A. Borzi, F. Weickert, A. J. Schofield, R. S. Perry, T. Tayama, T. Sakakibara, Y. Maeno, A. G. Green, and A. P. Mackenzie. Disorder-sensitive phase formation linked to metamagnetic quantum criticality. *Science*, 306:1154, 2004.

[11] R. A. Borzi, S. A. Grigera, J. Farrell, R. S. Perry, S. J. S. Lister, S. L. Lee, D. A. Tennant, Y. Maeno, and A. P. Mackenzie. Formation of a nematic fluid at high fields in sr3ru2o7. *Science*, 315:214, 2007.

[12] R. S. Perry, L. M. Galvin, S. A. Grigera, L. Capogna, A. J. Schofield, A. P. Mackenzie, M. Chiao, S. R. Julian, S. I. Ikeda, S. Nakatsuji, Y. Maeno, and C. Pfleiderer. Metamagnetism and critical fluctuations in high quality single crystals of the bilayer ruthenate $sr_3ru_2o_7$. *Phys. Rev. Lett.*, 86(12):2661–2664, Mar 2001.

[13] A. J. Millis, A. J. Schofield, G. G. Lonzarich, and S. A. Grigera. Metamagnetic quantum criticality. *Physical Review Letters*, 88:217204, 2002.

[14] F. Ronning, R. W. Hill, M. Sutherland, D. G. Hawthorn, M. A. Tanatar, J. Paglione, Louis Taillefer, M. J. Graf, R. S. Perry, Y. Maeno, and A. P. Mackenzie. Thermal conductivity in the vicinity of the quantum critical endpoint in sr3ru2o7. *PHYS.REV.LETT*, 97:067005, 2006.

[15] Carsten Honerkamp. Charge instabilities at the metamagnetic transition. *Physical Review B*, 72:115103, 2005.

[16] B. Binz, A. Vishwanath, and V. Aji. Theory of the helical spin crystal: A candidate for the partially ordered state of mnsi. *Phys. Rev. Lett.*, 96:207202, 2006.

[17] H. Y. Kee and E. H. Kim. Itinerant metamagnetism induced by electronic nematic order. *Phys. Rev. B*, 71:184402, 2005.

[18] H. Yamase and A. A. Katanin. Van hove singularity and spontaneous fermi surface symmetry breaking in sr3ru2o7. *J.PHYS.SOC.JPN.*, 76:073706, 2007.

[19] C. Puetter, H. Doh, and H. Y. Kee. Meta-nematic transitions in a bilayer system: application to the bilayer ruthenate. arXiv.org:0706.1069, 2007.

[20] Y. Kohsaka, C. Taylor, P. Wahl, A. Schmidt, Jhinhwan Lee, K. Fujita, J. W. Alldredge, K. McElroy, Jinho Lee, H. Eisaki, S. Uchida, D.-H. Lee, and J. C. Davis. How cooper pairs vanish approaching the mott insulator in $bi_2sr_2cacu_2o_{8+\delta}$. *Nature*, 454:1072, 2008.

[21] T. Hanaguri, Y. Kohsaka, J. C. Davis, C. Lupien, I. Yamada, M. Azuma, M. Takano, K. Ohishi, M. Ono, and H. Takagi. Quasiparticle interference and superconducting gap in ca2-xnaxcuo2cl2. *Nature Physics*, 3:865, 2007.

[22] Qiang-Hua Wang and Dung-Hai Lee. Quasiparticle scattering interference in high-temperature superconductors. *Phys. Rev. B*, 67:020511, 2003.

[23] A. V. Balatsky, I. Vekhter, and Jian-Xin Zhu. Impurity-induced states in conventional and unconventional superconductors. *Rev. Mod. Phys.*, 78:373, 2006.

[24] J. C. Davis. KITP conference of higher temperature superconductivity, unpublised.

[25] J. Lee, M. P. Allan, M. A. Wang, J. Farrell, S. A. Grigera, F. Baumberger, J. C. Davis, and A. P. MacKenzie. Heavy d-electron quasiparticle interference and real-space electronic structure of $Sr_3Ru_2O_7. NaturePhysics, 5 : 800 - -804, November 2009.$

[26] A. Tamai, M. P. Allan, J. F. Mercure, W. Meevasana, R. Dunkel, D. H. Lu, R. S. Perry, A. P. Mackenzie, D. J. Singh, Z.-X. Shen, and F. Baumberger. Fermi surface and van hove singularities in the itinerant metamagnet *sr*3*ru*2*o*7. *Phys. Rev. Lett.*, 101:026407, 2008.

[27] Wei-Cheng Lee, D. P. Arovas, and Congjun Wu. Quasiparticle interference in the unconventional metamagnetic compound *sr*3*ru*2*o*7. *Phys. Rev. B*, 81(18):184403, May 2010.

[28] T.-M. Chuang, M. P. Allan, Jinho Lee, Yang Xie, Ni Ni, S. L. Bud'ko, G. S. Boebinger, P. C. Canfield, and J. C. Davis. Nematic electronic structure in the "parent" state of the iron-based superconductor $ca(fe_1 - xco_x)_2as_2$. *Science*, 327:181, 2010.

[29] S. Raghu, A. Paramekanti, E. A. Kim, R. A. Borzi, S. Grigera, A. P. Mackenzie, and S. A. Kivelson. Microscopic theory of the nematic phase in sr$_3$ru$_2$o$_7$. *Physical Review B*, 79:214402, 2009.

[30] X.-L. Qi and S.-C. Zhang. Topological insulators and superconductors. *ArXiv e-prints*, August 2010.

[31] M. Z. Hasan and C. L. Kane. *Colloquium*: Topological insulators. *Rev. Mod. Phys.*, 82:3045–3067, Nov 2010.

[32] B. A. Bernevig, J. Orenstein, and S. C. Zhang. unpublished; cond-mat/0606196, 2006.

[33] C. L. Kane and E. J. Mele. z_2 topological order and the quantum spin hall effect. *Physical Review Letters*, 95:146802, 2005.

[34] C. L. Kane and E. J. Mele. Quantum spin hall effect in graphene. *Physical Review Letters*, 95:226801, 2005.

[35] B. Andrei Bernevig, Taylor L. Hughes, and Shou-Cheng Zhang. Quantum spin hall effect and topological phase transition in hgte quantum wells. *Science*, 314:1757, 2006.

[36] M. König, S. Wiedmann, C. Brüne, A. Roth, H. Buhmann, L. W. Molenkamp, X. L. Qi, and S. C. Zhang. *Science*, 318:766, 2007.

[37] L. Fu and C. L. Kane. Topological insulators with inversion symmetry. *Physical Review B*, 76:045302, 2007.

[38] Liang Fu and C. L. Kane. Superconducting proximity effect and majorana fermions at the surface of a topological insulator. arXiv.org:0707.1692, 2007.

[39] J. E. Moore and L. Balents. Topological invariants of time-reversal-invariant band structures. *Physical Review B*, 75:121306, 2007.

[40] X.-L. Qi, S. Raghu, C.-X. Liu, D. J. Scalapino, and S.-C. Zhang. arXiv.org:0804.4332, 2008.

[41] D. Hsieh, D. Qian, L. Wray, Y. Xia, Y. S. Hor, R. J. Cava, and M. Z. Hasan. A topological dirac insulator in a quantum spin hall phase. *Nature*, 452:970, 2008.

[42] D. Hsieh, Y. Xia, D. Qian, L. Wray, J. H. Dil, F. Meier, J. Osterwalder, L. Patthey, J. G. Checkelsky, N. P. Ong, A. V. Fedorov, H. Lin, A. Bansil, D. Grauer, Y. S. Hor, R. J. Cava, and M. Z. Hasan. A tunable topological insulator in the spin helical dirac transport regime. *Nature*, 460(9):1101, 2009.

[43] C. Wu, B. Andrei Bernevig, and S. C. Zhang. The helical liquid and the edge of quantum spin hall systems. *Physical Review Letters*, 96:106401, 2006.

[44] C. Xu and J. E. Moore. Stability of the quantum spin hall effect: effects of interactions, disorder, and z_2 topology. *Physical Review B*, 73:064417, 2006.

[45] Dong Zheng, Guang-Ming Zhang, and Congjun Wu. Particle-hole symmetry and interaction effects in the kane-mele-hubbard model. *Phys. Rev. B*, 84:205121, Nov 2011.

[46] M. Hohenadler, T. C. Lang, and F. F. Assaad. Correlation Effects in Quantum Spin-Hall Insulators: A Quantum Monte Carlo Study. *Physical Review Letters*, 106(10):100403–+, March 2011.

[47] J. E. Hirsch. Two-dimensional hubbard model: Numerical simulation study. *Phys. Rev. B*, 31:4403–4419, Apr 1985.

[48] Z. Y. Meng, T. C. Lang, S. Wessel, F. F. Assaad, and A. Muramatsu. Quantum spin liquid emerging in two-dimensional correlated Dirac fermions. , 464:847–851, April 2010.

[49] J. Kondo. Resistance minimum in dilute magnetic alloys. *Prog. Theor. Phys.*, 32:37, 1964.

[50] A. C. Hewson. *The Kondo Problem to Heavy Fermions*. Cambridge University Press, 1993.

[51] P. Coleman. Local moment physics in heavy electron systems. cond-mat/0206003, 2002.

[52] I. Affleck. Conformal field theory approach to the kondo effect. *ACTA PHYS.POLON.B*, 26:1869, 1995.

[53] M. Pustilnik and L. I. Glazman. Kondo effect in quantum dots. *Journal of Physics Condensed Matter*, 16:R513, 2004.

[54] P. Nozieres and A. Blandin. *Journal de Physique C*, 41:193, 1980.

[55] L. Kouwenhoven and L. Glazman. Revival of the kondo effect. *PHYSICS WORLD*, 14:33, 2001.

[56] C. Wu, B. A. Bernevig, and S. C. Zhang. The helical liquid and the edge of quantum spin hall systems. *Physical Review Letters*, 96:106401, 2006.

[57] J. Maciejko, C. Liu, Y. Oreg, X. L. Qi, Congjun Wu, and S.-C. Zhang. Kondo effect in the helical edge liquid of the quantum spin hall state. *Physical Review Letters*, 102:256803, 2009.

[58] F. D. M. Haldane. Model for a quantum hall effect without landau levels: Condensed-matter realization of the "parity anomaly". *Phys. Rev. Lett.*, 61(18):2015–2018, Oct 1988.

[59] Y. Li and C. Wu. Three Dimensional Topological Insulators with Landau Levels. *arXiv:1103.5422*, March 2011.

[60] Y. Li, K. Intriligator, Y. Yu, and C. Wu. Isotropic Landau levels of Dirac fermions in high dimensions. *ArXiv e-prints*, August 2011.

[61] Y. Kamihara, T. Watanabe, M. Hirano, and H. Hosono. Iron-based layered superconductor la[o1-xfx]feas (x = 0.05-0.12) with tc = 26 k. *Journal of the American Chemical Society*, 130(11):3296–3297, 2008.

[62] X. H. Chen, T. Wu, G. Wu, R. H. Liu, H. Chen, and D. F. Fang. Superconductivity at 43 k in smfeaso1-xfx. *Nature*, 453:761, 2008.

[63] G. F. Chen, Z. Li, D. Wu, G. Li, W. Z. Hu, J. Dong, P. Zheng, J. L. Luo, and N. L. Wang. Superconductivity at 41 k and its competition with spin-density-wave instability in layered ceo1-xfxfeas. *Phys. Rev. Lett.*, 100:247002, 2008.

[64] H. H. Wen, G. Xu, L. Fang, H. Yang, and X. Zhu. *Europhys. Lett.*, 82:17009, 2008.

[65] Z. A. Ren, G.-C. Che, X.-L. Dong, J. Yang, W. Lu, W. Yi, X.-L. Shen, Z.-C. Li, L.-L. Sun, F. Zhou, and Z.-X. Zhao. Superconductivity and phase diagram in iron-based arsenic-oxides refeaso1-(b (re = rare-earth metal) without fluorine doping. *Europhys. Lett.*, 83:17002, 2008.

[66] M. Rotter, M. Tegel, I. Schellenberg, W. Hermes, R. Pottgen, and D. Johrendt. Spin density wave anomaly at 140 k in the ternary iron arsenide bafe2as2. *Phys. Rev. B*, 78:020503, 2008.

[67] C.-C Joseph Wang, Bhagawan Sahu, Hongki Min, Wei-Cheng Lee, and Allan H. MacDonald. Quantum wells in polar-nonpolar oxide heterojunction systems. arXiv.org:0810.0798, 2008.

[68] I.I. Mazin, D.J. Singh, M.D. Johannes, and M.H. Du. Unconventional superconductivity with a sign reversal in the order parameter of lafeaso$_{1-x}$f$_x$. *Phys. Rev. Lett.*, 101:057003, 2008.

[69] K. Kuroki, S. Onari, R. Arita, H. Usui, Y. Tanaka, H. Kontani, and H. Aoki. Unconventional pairing originating from the disconnected fermi surfaces of superconducting lafeaso$_{1-x}$f$_x$. *Phys. Rev. Lett.*, 101:087004, 2008.

[70] D. Parker, O. V. Dolgov, M. M. Korshunov, A. A. Golubov, and I. I. Mazin. arXiv.org:0807.3729, 2008.

[71] A. V. Chubukov, D. Efremov, and I. Eremin. superconductors. arXiv.org:0807.3735, 2008.

[72] Yunkyu Bang and Han-Yong Choi. arXiv.org:0808.0302, 2008.

[73] H. Luetkens, H. H. Klauss, R. Khasanov, A. Amato, R. Klingeler, I. Hellmann, N. Leps, A. Kondrat, C. Hess, A. Kohler, G. Behr, J. Werner, and B. Buchner. arXiv.org:0804.3115, 2008.

[74] L. Malone, J. D. Fletcher, A. Serafin, A. Carrington, N. D. Zhigadlo, Z. Bukowski, S. Katrych, and J. Karpinski. arXiv.org:0806.3908, 2008.

[75] K. Hashimoto, T. Shibauchi, T. Kato, K. Ikada, R. Okazaki, H. Shishido, M. Ishikado, H. Kito, A. Iyo, H. Eisaki, S. Shamoto, and Y. Matsuda. arXiv.org:0806.3149, 2008.

[76] W. Q. Chen, K. Y. Yang, Y. Zhou, and F.-C. Zhang. arXiv.org:0808.3234, 2008.

[77] Kazuhiko Kuroki, Hidetomo Usui, Seiichiro Onari, Ryotaro Arita, and Hideo Aoki. Pnictogen height as a possible switch between high-t_c nodeless and low-t_c nodal pairings in the iron based superconductors. *Physical Review B*, 79:224511, 2009.

[78] Wei-Cheng Lee, Shou-Cheng Zhang, and Congjun Wu. Pairing state with a time-reversal symmetry breaking in feas-based superconductors. *Physical Review Letters*, 102(21):217002, 2009.

[79] Jing Xia, Yoshiteru Maeno, Peter T. Beyersdorf, M. M. Fejer, and Aharon Kapitulnik. High resolution polar kerr effect measurements of sr2ruo4: Evidence for broken time-reversal symmetry in the superconducting state. *Phys. Rev. Lett.*, 97:167002, 2006.

[80] B. Fauqué, Y. Sidis, V. Hinkov, S. Pailhès, C. T. Lin, X. Chaud, and P. Bourges. Magnetic order in the pseudogap phase of high-t[sub c] superconductors. *Phys. Rev. Lett.*, 96(19):197001, 2006.

[81] C. M. Varma and L. J. Zhu. Helicity order: Hidden order parameter in uru2si2. *Phys. Rev. Lett.*, 96:036405, 2006.

[82] Vivek Aji and C. M. Varma. Theory of the quantum critical fluctuations in cuprate superconductors. *Phys. Rev. Lett.*, 99(6):067003, 2007.

[83] Can-Li Song, Yi-Lin Wang, Peng Cheng, Ye-Ping Jiang, Wei Li, Tong Zhang, Zhi Li, Ke He, Lili Wang, Jin-Feng Jia, Hsiang-Hsuan Hung, Congjun Wu, Xucun Ma, Xi Chen, and Qi-Kun Xue. Direct observation of nodes and twofold symmetry in fese superconductor. *Science*, 332(6036):1410–1413, 2011.

[84] H.-H. Hung, C.-L. Song, X. Chen, X. Ma, Q.-k. Xue, and C. Wu. Anisotropic vortex lattice structures in the FeSe superconductor. *ArXiv:1109.6116*, September 2011.

[85] Wei-Cheng Lee, Congjun Wu, Daniel P. Arovas, and Shou-Cheng Zhang. Quasiparticle interference on the surface of the topological insulator *bi*2*te*3. *Phys. Rev. B*, 80(24):245439, Dec 2009.